

Project No: 603502

DACCIWA

"Dynamics-aerosol-chemistry-cloud interactions in West Africa"

Deliverable

D 5.4 Radiation closure

<u>Due date of deliverable:</u>	30/11/2017		
<u>Completion date of deliverable:</u>	30/11/2017		
Start date of DACCIWA project:	1 st December 2013	Project duration:	60 months
Version:	[V1.0]		
File name:	[D_5.4_RadiationClosure_v1.0.pdf]		
Work Package Number:	5		
Task Number:	4		
<u>Responsible partner for deliverable:</u>	UREAD		
Contributing partners:			
Project coordinator name:	Prof. Dr. Peter Knippertz		
Project coordinator organisation name:	Karlsruher Institut für Technologie		

The DACCIWA Project is funded by the European Union's Seventh Framework Programme for research, technological development and demonstration under grant agreement no 603502.

Dissemination level		
PU	Public	x
PP	Restricted to other programme participants (including the Commission Services)	
RE	Restricted to a group specified by the consortium (including the Commission Services)	
CO	Confidential, only for members of the consortium (including the Commission Services)	

Nature of Deliverable		
R	Report	x
P	Prototype	
D	Demonstrator	
O	Other	

Copyright

This Document has been created within the FP7 project DACCIWA. The utilization and release of this document is subject to the conditions of the contract within the 7th EU Framework Programme. Project reference is FP7-ENV-2013-603502.

DOCUMENT INFO**Authors**

Author	Beneficiary Short Name	E-Mail
Peter Hill	UREAD	p.g.hill@reading.ac.uk
Christine Chiu	UREAD	c.j.chiu@reading.ac.uk
Richard Allan	UREAD	r.p.allan@reading.ac.uk

Changes with respect to the DoW

Issue	Comments

Dissemination and uptake

Target group addressed	Project internal / external
Scientific	Internal and external

Document Control

Document version #	Date	Changes Made/Comments
V0.1	17.11.2017	First version for approval by the general assembly
V1.0	30.11.2017	Final version after approval by the general assembly

Table of Contents

1	Introduction	5
2	Methods	5
2.1	The SEVIRI OCA product	5
2.2	Irradiance measurements on aircraft during the DACCIWA field campaign.....	6
2.3	GERB data	8
2.4	Radiative transfer calculations	8
3	Evaluating SEVIRI OCA using radiative closure and aircraft irradiance measurements	9
3.1	Twin Otter flight 8 July a.m.....	9
3.2	SAFIRE flight 15 July a.m.	13
4	Summary and further work	14
5	References	15

1 Introduction

One of the aims of the DACCIWA project (Knippertz, et al., 2015) is to improve understanding of clouds in southern West Africa, particularly low clouds, which are difficult to observe from satellites (van der Linden, et al., 2015) and poorly represented in climate models (Hannak, et al., 2017).

Many cloud observations have been taken as part of the DACCIWA field campaign (Flamant, et al., 2017) and provide an invaluable resource for understanding cloud processes in the region. Yet satellite observations remain essential, due to the broader spatial and temporal context they provide. Moreover, the aircraft and ground-based observations made during the DACCIWA field campaign can be used to evaluate existing satellite cloud products and identify where improvements are required.

Radiative closure provides one method for evaluating cloud properties and will be the focus of this report. Radiative closure involves comparing measured irradiances with those predicted by a radiative transfer model. Since radiative transfer theory is well understood, radiative transfer models are very accurate and differences between the measured and predicted irradiances can be attributed to the input to the radiative transfer calculation, in particular the input cloud properties.

In this report we describe how radiative closure is used to evaluate the Spinning Enhanced Visible and Infrared Imager (SEVIRI) Optimal Cloud Analysis (OCA) product. We focus on this particular cloud product because of its potential usefulness in the DACCIWA region, as detailed in section 3.1.

2 Methods

2.1 The SEVIRI OCA product

The Spinning Enhanced Visible and Infrared Imager (SEVIRI) is a series of instruments on board the geostationary Meteosat Second Generation (MSG) satellites. Sitting above the intersection of the equator and the prime meridian, results in excellent diurnal sampling (15 minutes) and high resolution for the DACCIWA region (approx. 3 km). SEVIRI has 12 channels, four in the visible and near-infrared and eight in the infrared.

The optimal cloud analysis (OCA) product Watts (2011) uses an optimal estimation framework to retrieve clouds properties from all SEVIRI channels simultaneously for up to two cloud layers. The optimal estimation framework ensures that the retrieved cloud properties are physically consistent with each other and results in well-defined uncertainty estimates for each variable. Attempting to retrieve multi-layer cloud properties from passive satellite measurements is rather novel and to our knowledge has this aspect of the retrieval is unique. Clearly this is potentially very useful for the DACCIWA region where multi-layer cloud is common and low cloud is often obscured by higher cloud (Stein, et al., 2011; van der Linden, et al., 2015). Multi-layer cloud retrievals may also lead to better estimates of the cloud top height for the upper layer, which is often underestimated when lower cloud is present. The OCA product provides estimates of cloud top pressure and optical thickness for up to two layers and cloud effective radius and phase for the upper layer.

The OCA product has enormous potential for the DACCIWA region, but as a relatively new product, its performance is uncertain. By comparing the OCA product to observations taken during the field campaign we aim to assess its usefulness for understanding cloud processes in this region and highlight avenues for potential improvement in future retrievals.

2.2 Irradiance measurements on aircraft during the DACCIWA field campaign

Both the French Service des Avions Français Instrumentés pour la Recherche en Environnement (SAFIRE) ATR42 and the British Antarctic Survey (BAS) Twin Otter aircraft were equipped with two pyranometers measuring solar irradiance and two pyrgeometers measuring thermal irradiance during the DACCIWA field campaign. One of each instrument was positioned above the aircraft pointing upwards to measure downwelling irradiances and the other was positioned below the aircraft pointing downwards to measure upwelling irradiances.

The ATR42 was equipped with two Kipp & Zonen CMP22 pyranometers, which have an uncertainty of approximately 5 W m^{-2} and a response time of two seconds and two Kipp & Zonen PGR4 pyrgeometers, which have an uncertainty of approximately 4 W m^{-2} and a response time of six seconds. The Twin Otter was equipped with two Eppley labs PSP pyranometers, which have an uncertainty of 10 W m^{-2} and a response time of one second and two Eppley labs PIR pyrgeometers, which have an uncertainty of approximately 5 W m^{-2} and a response time of two seconds.

Downwelling solar irradiances have a large direct beam component, which means that the measured irradiance is strongly dependent on the angle of the pyranometer relative to the sun. For comparison with radiative transfer calculations, we require the downwelling solar irradiance through a horizontal plane parallel to the earth's surface. This can be calculated from the measured downwelling solar irradiance using the following equation

$$F_{corr} = \frac{F(\beta)}{1 - f \cdot \left(1 - \frac{\cos\beta}{\cos\theta}\right)}$$

where F_{corr} is the corrected flux through the horizontal plane, $F(\beta)$ is the measured flux, f is the ratio of direct to total irradiance, θ is the solar zenith angle and β is the angle between the normal to the top of the aircraft and the direct sunbeam, which is calculated as

$$\cos(\beta) = (\cos(r_{air} + r_{pyr}) \cdot \cos(p_{air} + p_{pyr}) \cdot \cos\theta) - (\cos(r_{air} + r_{pyr}) \cdot \sin(p_{air} + p_{pyr}) \cdot \cos\varphi) - (\sin(r_{air} + r_{pyr}) \cdot \sin\theta \cdot \sin\varphi)$$

where r_{air} is the aircraft roll angle, r_{pyr} is the roll offset angle of the pyranometer from the aircraft, p_{air} is the aircraft pitch angle, p_{pyr} is the pitch offset angle of the pyranometer from the aircraft, and φ is the difference between the aircraft heading and the solar azimuth angle. The aircraft pitch and roll angles are measured on the aircraft. The solar zenith and azimuth angles can be calculated from the time and location of the aircraft, both of which are measured by the aircraft. However, the ratio of direct to total irradiance, and the pitch and roll offset angles of the pyranometers relative to the aircraft are unknown. The pitch and roll offset angles arise from the fact that the pyranometers may not be attached exactly parallel to the geometrical plane of the aircraft. They are likely to be small, but even so may lead to significant differences in the calculation of F_{corr} .

To estimate the pyranometer pitch and roll offset angles, one calibration flight was performed with each aircraft. In these calibration flights the aircraft flew above cloud at a variety of angles relative to the sun. As the aircraft were above cloud, the atmosphere above the aircraft is expected to be homogeneous and optically thin. As a result, f can be estimated reasonably well and F_{corr} should be approximately constant for the whole flight once it has been normalized to account for changes

in the solar zenith angle. This means that we can estimate p_{pyr} and r_{pyr} as those angles that minimize the changes in the normalized value of F_{corr} as the aircraft changes direction.

The Twin Otter calibration flight took place on 15 July. Figure 1 illustrates how this flight was used to estimate p_{pyr} and r_{pyr} . The aircraft flew three box patterns, flying towards the sun in the first leg, with the sun to the left of the aircraft for the second leg, flying away from the sun for the third leg and flying with the sun to the right of the aircraft for the fourth leg. After these three box patterns, the aircraft then flew at 45 degrees to the sun while varying the pitch of the aircraft. When the pitch or roll angle of the aircraft is very large, the pyranometer will detect upwelling shortwave irradiance, which is not accounted for in our correction. Consequently, we do not count points where the pitch or roll angle exceeds 10° . The resulting normalized irradiance measurements (black lines) show clear systematic changes between the different legs of the flight, with a standard deviation of 22.74 W m^{-2} . Assuming p_{pyr} and r_{pyr} are zero, the corrected normalized irradiance (red line) has a smaller standard deviation of 15.50 W m^{-2} with smaller differences between the different legs of the flight. We found that of $p_{pyr}=0.15^\circ$ and $r_{pyr}=1.86^\circ$ resulted in a minimum standard deviation (13.27) for the corrected normalized irradiance. Figure 1 assumes that 95 % of the total irradiance is direct beam. We also calculated p_{pyr} and r_{pyr} using values of 91 % and 99 % and calculated p_{pyr} and r_{pyr} independently for each of the three boxes that make up the flight. This results in 12 estimates of p_{pyr} and r_{pyr} in total. For other Twin Otter flights, corrected irradiances are calculated with all twelve values and the differences are used as a measure of uncertainty due to the correction.

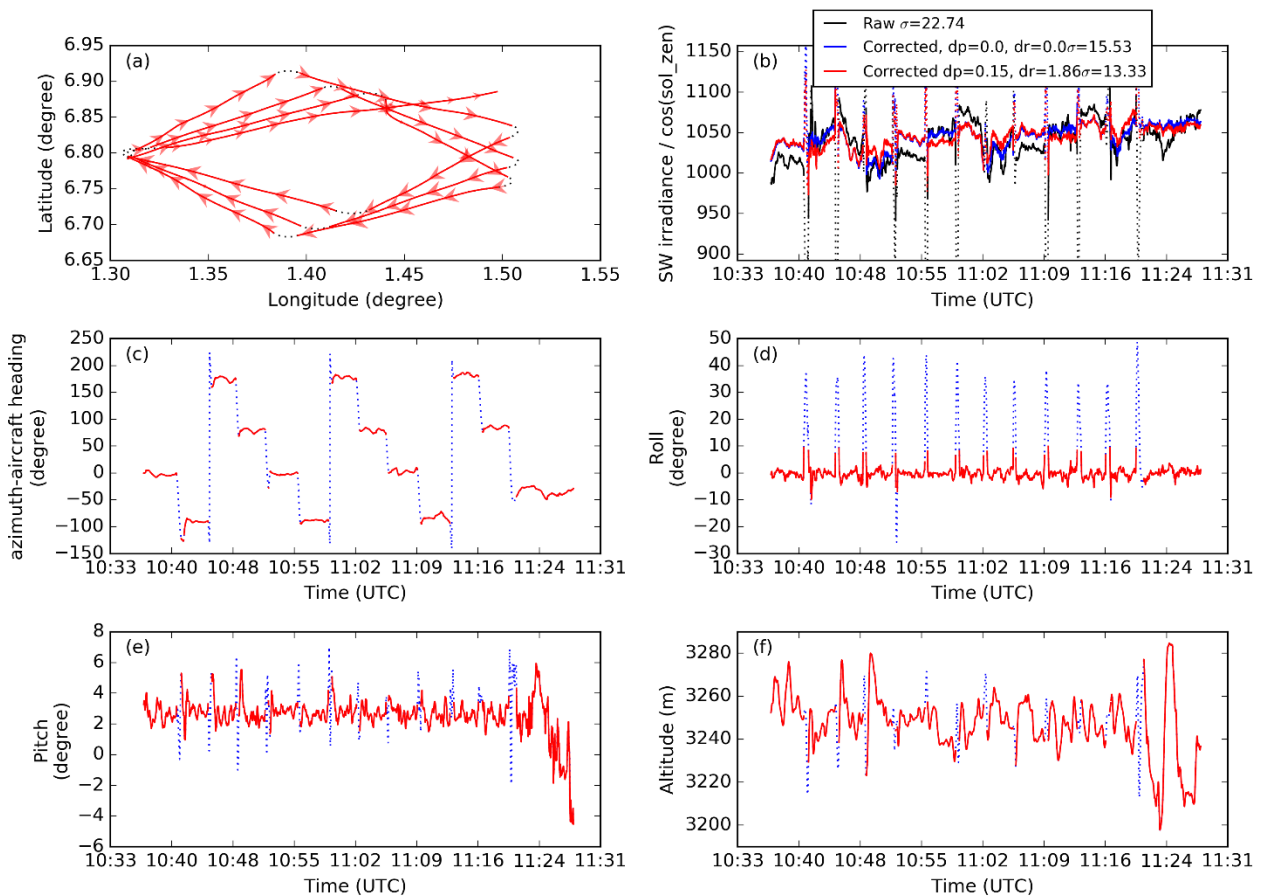


Figure 1 Flight pattern, normalized corrected solar downwelling irradiance, and aircraft angles for the Twin Otter flight on 15 July.

A similar flight pattern was also used with the ATR42 to derived pitch and roll offset angles for that aircraft, which are applied in the same way as they are for the Twin Otter.

2.3 GERB data

Geostationary Earth Radiation Budget (GERB) measurements (Harries, et al., 2005; Dewitte, et al., 2008) provide a coincident estimate of the top of atmosphere outgoing solar and thermal irradiance. GERB3 was launched in October 2012 and calibration and validation activities are ongoing. As a result it is not currently recommended for science use. Instead we use the GL (GERB-like) dataset derived from the SEVIRI instrument. In particular, we use the high-resolution (HR) product that has a temporal resolution of 15 minutes and a horizontal resolution of 9 km at nadir.

For each aircraft irradiance measurement, we identify the 8 surrounding GERB measurements in space and time and use linear interpolation to estimate a top of atmosphere irradiance corresponding to the aircraft location. The 8 surrounding GERB measurements are then used as a measure of uncertainty in the top of atmosphere irradiances due to spatial and temporal variability.

2.4 Radiative transfer calculations

Radiative transfer calculations use the Suite Of Community RAdiative Transfer codes based on Edwards and Slingo (SOCRATES). We conduct a radiative transfer calculation for each aircraft measurement. Vertical pressure levels, and temperature and humidity profiles are based on the ERA5 reanalysis hourly analyses. Aerosol properties are taken from the CAMS reanalysis and linearly interpolated onto ERA5 vertical levels. To account for cloud spatial variability, we identify the 27 closest OCA observations in space and time (i.e. the 3x3 nearest in space and for the 3 nearest times), do a radiative transfer calculation for each of these OCA retrievals and then linearly interpolate the resulting irradiances. The spread in the 27 calculated irradiances is used as a measure of uncertainty due to spatial and temporal variability. The OCA product provides cloud top pressure and cloud optical thickness for both layers, but not cloud physical thickness. We estimate this from the cloud optical depth using equation (2) from Chiu, et al. (2014). Once the cloud thickness has been determined, the cloud extinction is assumed to be constant throughout the cloud. Cloud phase is not retrieved for the second OCA layer (if present), so we estimate this using the layer temperature. We designate the cloud as liquid if the temperature is above 273.15 K, ice if the temperature is below 233.15 K and assign the cloud extinction to each phase by linearly scaling between these temperatures. For ice cloud, an estimate of the ice water content is calculated from the extinction and temperature by inverting the ice single scattering properties parametrization (Baran, et al., 2013) used in the atmospheric radiative transfer calculations. For liquid clouds, the cloud effective radius when not provided by OCA (i.e. for second cloud layers) is assumed to be 7 microns. Then the liquid water content is calculated as two thirds of the product of the extinction and the effective radius. Liquid single scattering properties are parametrized in the radiation calculations as described in Edwards & Slingo (1996). Ice cloud single scattering properties are parametrized as a function of temperature and ice water content as described by Baran, et al. (2013).

3 Evaluating SEVIRI OCA using radiative closure and aircraft irradiance measurements

3.1 Twin Otter flight 8 July a.m.

This flight took place in Togo, close to the Benin border on 8 July for the purpose of radiation closure, with a low cloud between 600 and 860 metres above the surface. Figure 2 shows the aircraft position and where cloud water content measurements from the Cloud Droplet Probe (CDP) on the twin otter exceed 0.01 g m^{-2} . The aircraft initially flew from South to North then North-East to South-West below cloud (Fig. 2 (b)), before climbing through the cloud while flying from South-West to North-East and returning to the South-West above cloud (Fig. 2 (c)). The aircraft then descended below cloud, flew to the North and repeated the legs above and below cloud along a North-West to South-East transect (Fig. 2 (d)). This flight pattern aimed to ensure sufficient radiation measurements were made both above and below the cloud layer, over as small region and time period as possible, to minimize changes in the cloud layer.

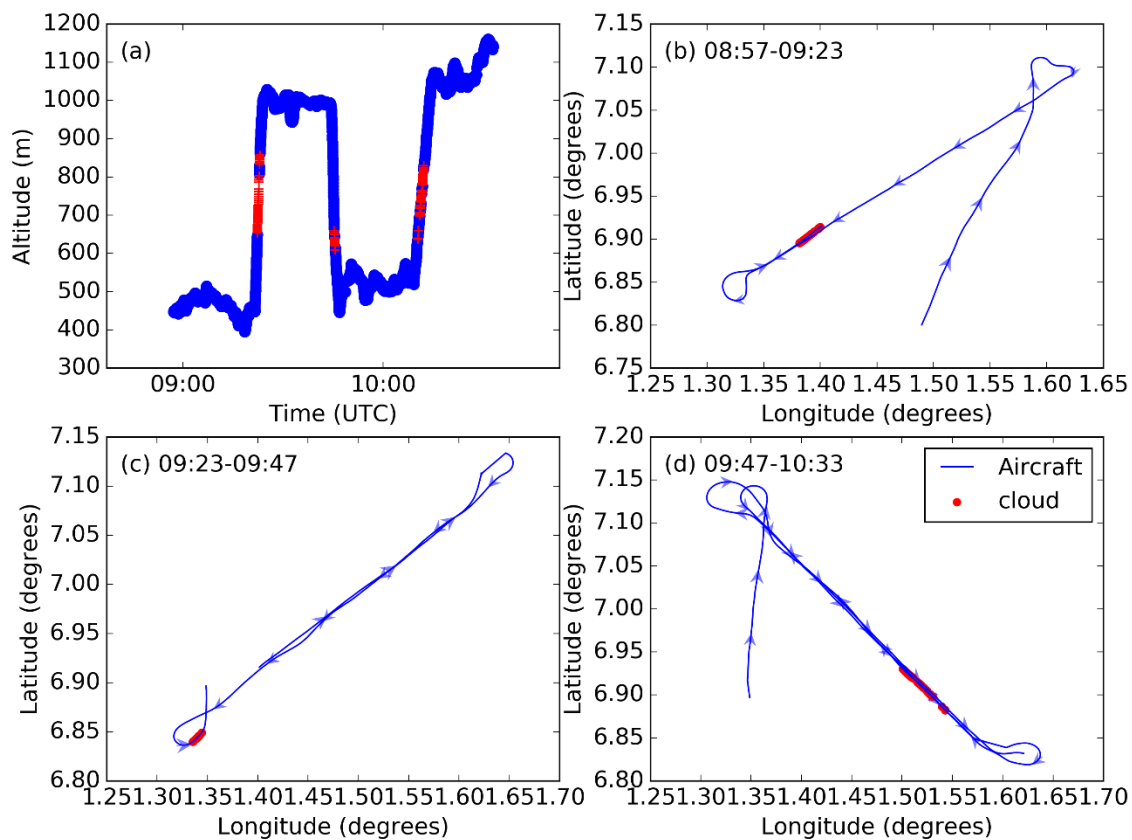


Figure 2 Location of the twin otter aircraft and where the CDP detected cloud for the 8 July a.m. flight. (a) shows the vertical location of the aircraft and cloud. (b), (c) and (d) show the aircraft location and flight direction together with non-zero cloud measurements for the first leg below cloud, the first leg above cloud and the second legs above and below cloud, respectively.

Figure 3 shows the location of the OCA cloud in the nearest SEVIRI pixel to the aircraft. The cloud top pressure comes directly from the OCA product, while the cloud physical thickness is determined from the optical depth following equation (2) in Chiu, et al. (2014). At the start of the flight, the OCA product retrieves two cloud layers. The upper layer has a relatively constant cloud top pressure of around 220 hPa. The lower layer has a more varied cloud top between 300 and 900 hPa. From approx. 9.40 onwards, both layers become less homogeneous, with pixels where only one cloud layer is identified. The OCA product shows no indication of the layer between 600 and 860 metres (approx. 925 and 960 hPa).

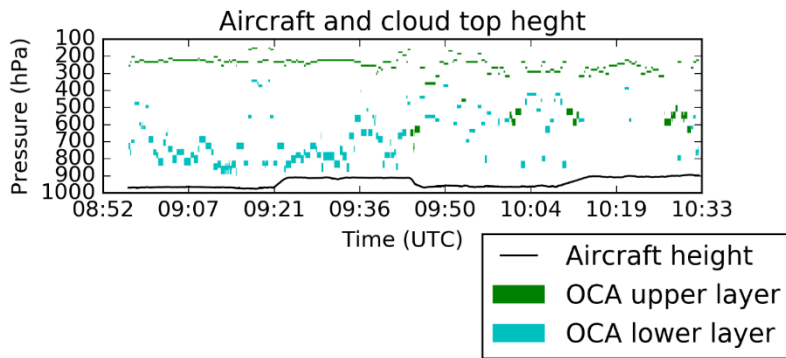


Figure 3 Altitude of aircraft and location of OCA cloud for the nearest SEVIRI pixel to the aircraft

Figure 4 compares calculated and measured irradiances for this flight. Outgoing top of atmosphere irradiances agree well, which suggests that the upper layer cloud top height and total cloud optical depth are reasonable. SW downwelling measurements are rather noisy, which dwarfs differences between the measured and calculated irradiances. However, there is a very strong signal for the missing low cloud in the SW upwelling irradiances. When the aircraft is above the low cloud, there is a large increase in the measured upwelling SW irradiance, due to reflection from the cloud below. For the calculated irradiances, where the low cloud is missing, there is no increase in upwelling SW irradiance at these times.

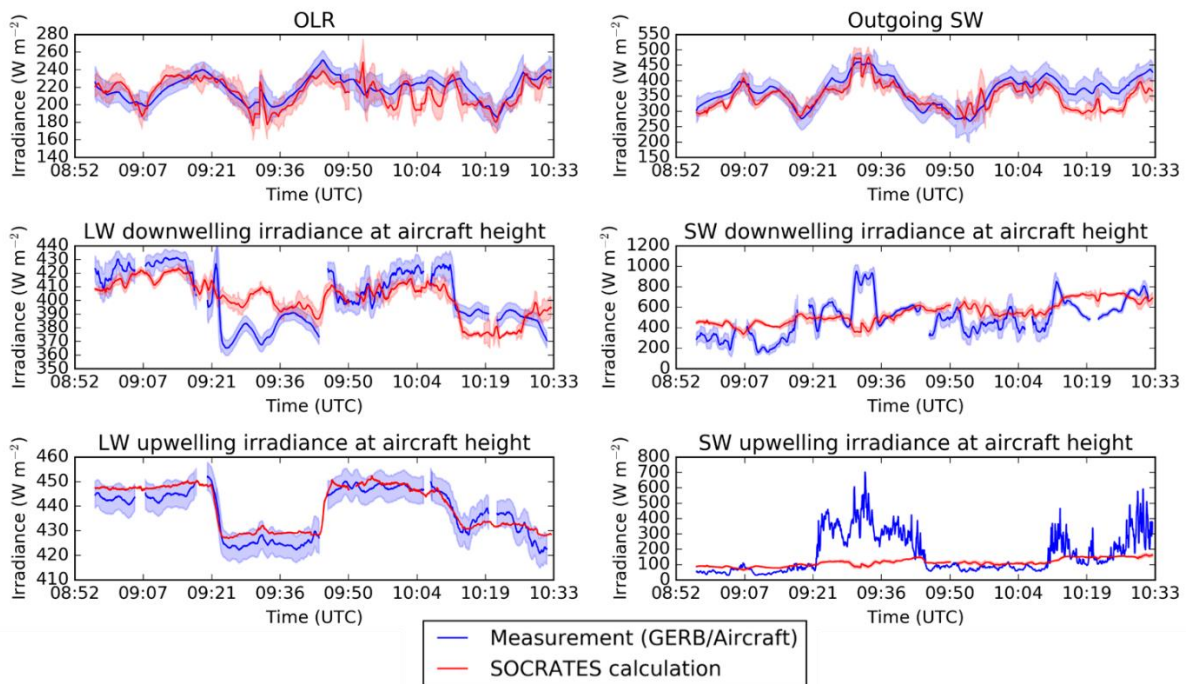


Figure 4 Comparison of measured and calculated irradiance for the Twin Otter flight on 8 July a.m. Blue lines show measurements from GERB at the top of atmosphere and the aircraft. Red lines show calculated irradiances at the same heights.

There are two possible reasons that the low cloud is missing in the SEVIRI OCA product. One possibility is that there are three cloud layers in reality and this lowest layer is not identified because the SEVIRI OCA algorithm identifies a maximum of two cloud layers. The other possibility is that there are two cloud layers in reality and the SEVIRI OCA retrieval overestimates the height of the lower layer. To test these two hypotheses, we run two further radiative transfer calculations, where we change the cloud used in the calculations, as shown in Fig. 5. In the first (Fig. 5(a)), we add an additional cloud layer where the CDP measurements indicate cloud should be present. In the second (Fig. 5(b)), we lower the second cloud layer to the layer where CDP measurements indicate cloud should be present.

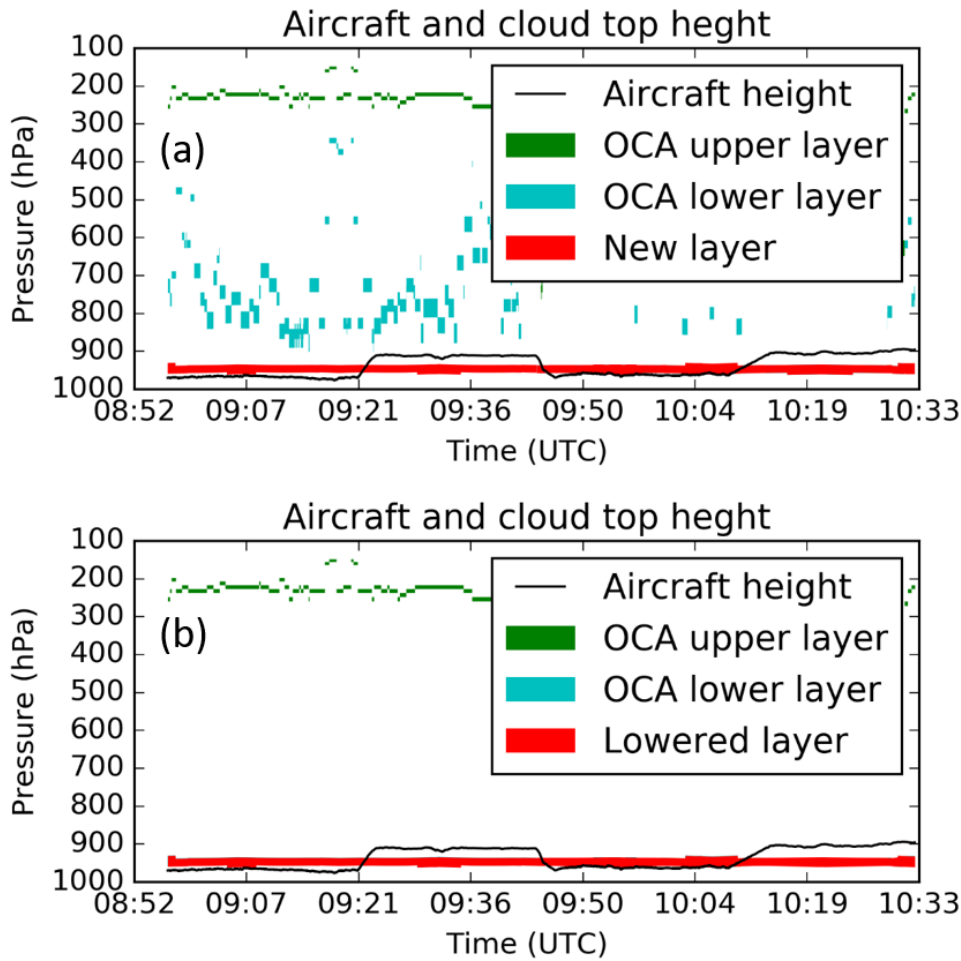


Figure 5. Location of cloud relative to the aircraft for the two new calculations for the Twin Otter 8 July a.m. flight (a) where an additional cloud layer is added where at the altitudes where the aircraft detects cloud and (b) where cloud with top below 300 hPa is lowered to the altitude where the aircraft detects cloud.

Fig. 6 compares the irradiances from these two new calculations and the original calculation with the measured irradiances. Both of the new calculations generally show a better agreement with the observations than the original calculation, which is particularly evident for the SW upwelling irradiance at the aircraft height. The calculation where the cloud is lowered is a better match to the SW upwelling irradiance than the one where we add an additional cloud layer, which suggests that in reality there is most likely only two cloud layers and the OCA product overestimates the height of the lower layer.

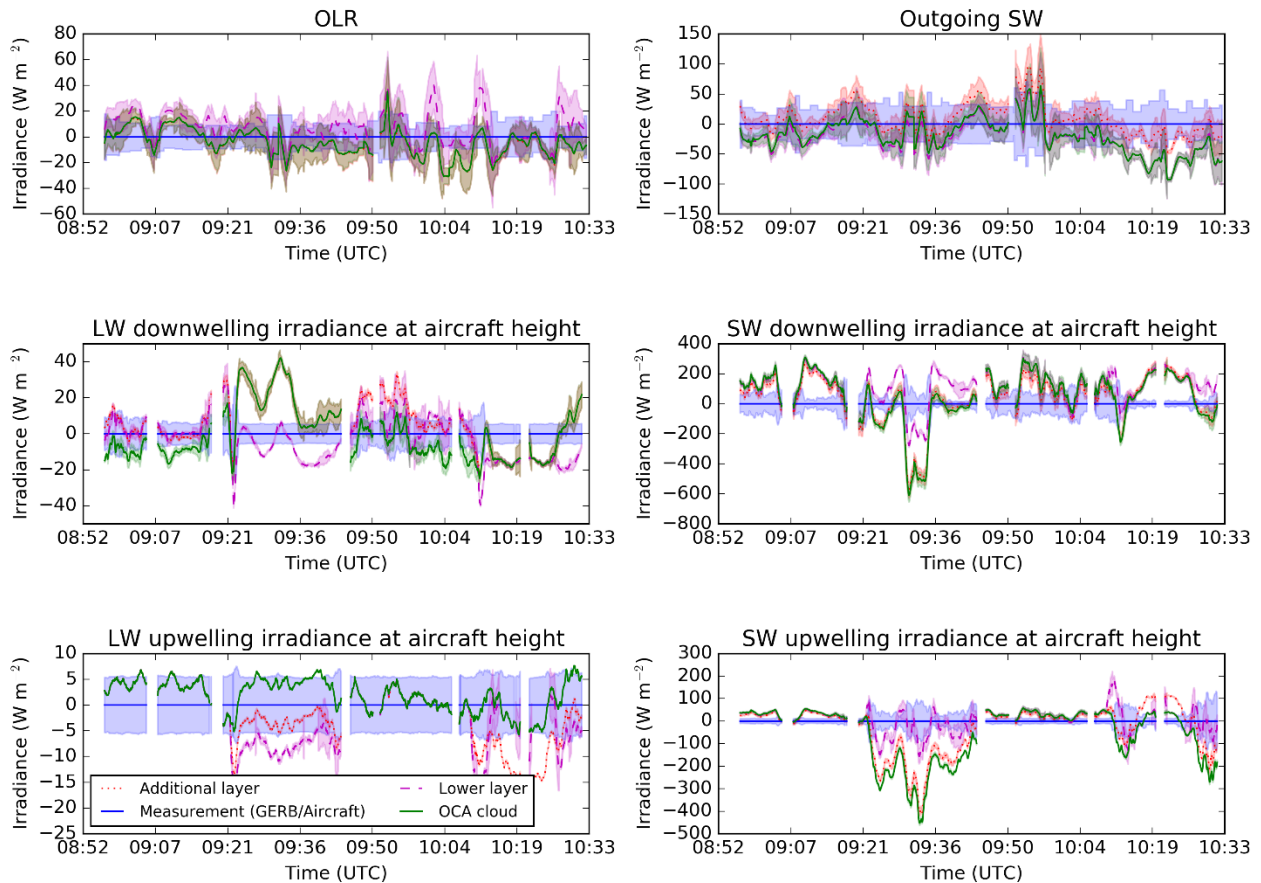


Figure 6 Difference between the calculated and observed irradiances for the three radiative transfer calculations conducted for the Twin Otter 8 July a.m. flight.

3.2 SAFIRE flight 15 July a.m.

The SAFIRE flight on 15 July was also aimed at radiative closure, with manoeuvres taking place over the surface supersite at Save. This involved flying repeated triangle patterns, with legs above, below and within cloud as shown in Fig. 7.

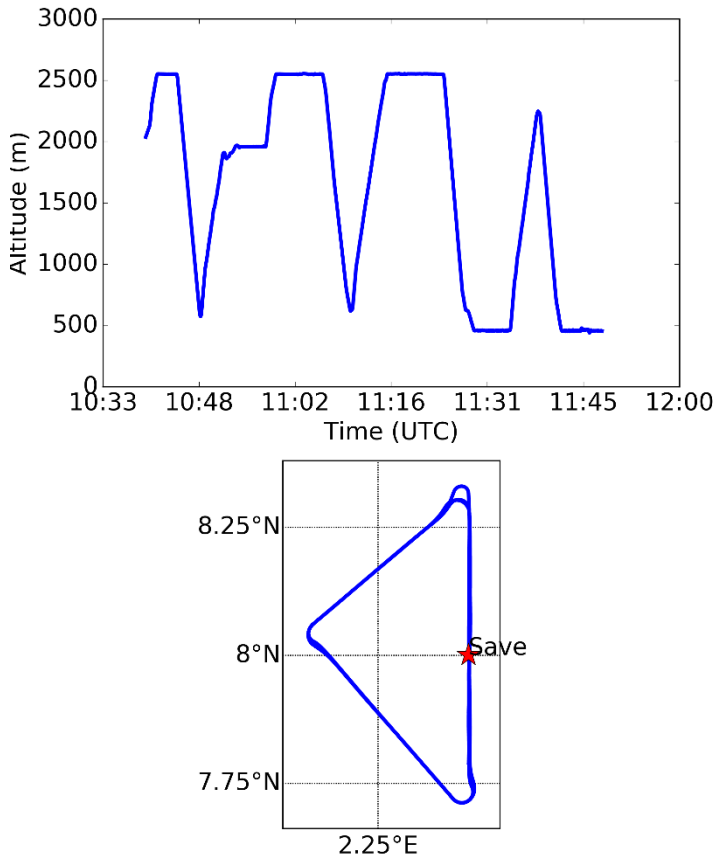


Figure 7 Flight pattern for the radiative closure manoeuvres conducted during the ATR42 flight on 15 July. The upper plot shows the aircraft altitude as a function of time and the lower plot shows the path the aircraft flew along and the location of the Save supersite

Figure 8 shows the calculated and measured irradiances for these manoeuvres along with the aircraft location and the location of the retrieved OCA cloud in the nearest SEVIRI pixels. The OCA retrieval generally places cloud between the altitudes that the aircraft flew at, though occasionally it identifies cloud outside these altitudes. The calculated irradiances generally show good agreement with the measured values. However, the outgoing longwave radiation predicted by the calculations is consistently around 10 W m^{-2} lower in the calculations than observed. This suggests the cloud top may be a little too high in the calculations, which is similar to the error for the Twin Otter 15 July flight.

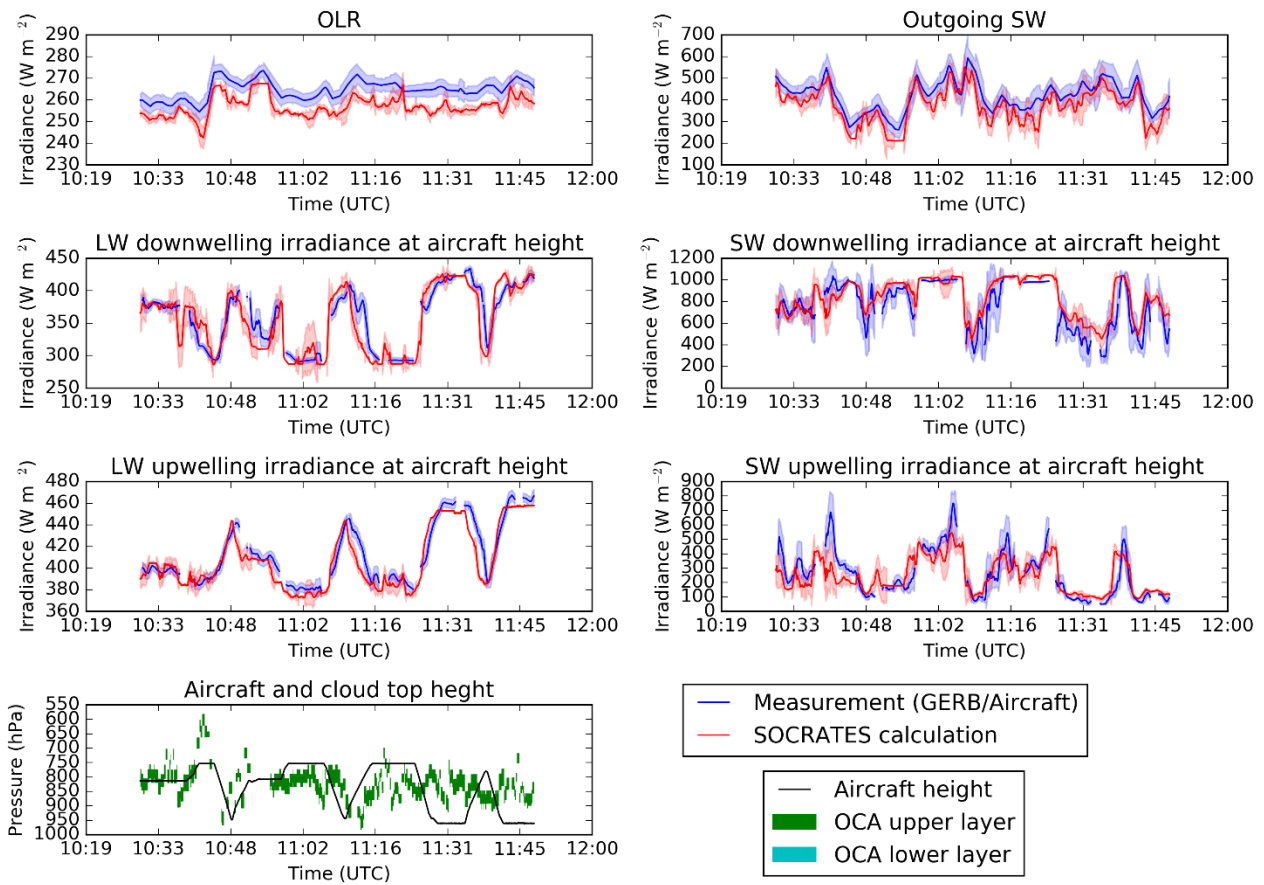


Figure 8 Comparison of modelled and measured irradiances for the ATR42 radiative closure flight on 15 July. Blue lines show measurements and red lines show calculated irradiances. The bottom left panel shows the location of the aircraft and the OCA retrieved cloud in the nearest SEVIRI pixel.

4 Summary and further work

We have demonstrated how radiative closure can be used to identify errors in satellite cloud retrievals, in particular the SEVIRI OCA product. We have focused on two particular case studies. The first, is based on a twin otter flight on 8 July, where radiative closure suggests that cloud top height for a second cloud layer is far too high in the SEVIRI OCA product. The second case study is based on a SAFIRE flight on 15 July. This case is perhaps more straightforward for the retrieval as there appears to be only a single cloud layer, and the OCA products does an excellent job of capturing the true cloud, resulting in very good agreement between the calculated and measured irradiances.

Future work will use radiative closure to evaluate the OCA retrieval for other flights during the DACCIWA field campaign. We shall also compare the aircraft and surface cloud measurements to the OCA retrieval in order to obtain a holistic view of the performance of the OCA retrieval in the DACCIWA region.

5 References

Baran, A. J. et al., 2013. A new high- and low-frequency scattering parameterization for cirrus and its impact on a high-resolution numerical weather prediction model. *AIP Conf. Proc.*, Volume 1531, pp. 716-719.

Chiu, J. C., Holmes, J. A., Hogan, R. J. & O'Connor, E. J., 2014. {The interdependence of continental warm cloud properties derived from unexploited solar background signals in ground-based lidar measurements}. *{Atmospheric Chemistry and Physics}*, {14}({16}), pp. {8389-8401}.

Dewitte, S. et al., 2008. The Geostationary Earth Radiation Budget Edition 1 data processing algorithms. *Advances in Space Research*, 41(11), pp. 1906-1913.

Edwards, J. M. & Slingo, A., 1996. Studies with a flexible new radiation code. 1: Choosing a configuration for a large-scale model. *Q. J. Roy. Meteorol. Soc.*, Volume 122, pp. 690-719.

Flamant, C. et al., 2017. {The Dynamics-Aerosol-Chemistry-Cloud Interactions in West Africa field campaign: Overview and research highlights}. *{Bull. Amer. Meteor. Soc.}*, Volume In press.

Hannak, L. et al., 2017. {Why Do Global Climate Models Struggle to Represent Low-Level Clouds in the West African Summer Monsoon?}. *{Journal of Climate}*, {30}({5}), pp. {1665-1687}.

Harries, J. E. et al., 2005. The Geostationary Earth Radiation Budget Project. *Bull. Amer. Meteor. Soc.*, 86(7), pp. 945-960.

Knippertz, P. et al., 2015. {The DACCIWA project: Dynamics-aerosol-chemistry-cloud interactions in West Africa}. *Bull. Amer. Meteor. Soc.*.

Stein, T. H. M. et al., 2011. The vertical cloud structure of the West African monsoon: A 4 year climatology using CloudSat and CALIPSO. *J. Geophys. Res.*, 116(D22).

van der Linden, R., Fink, A. H. & Redl, R., 2015. Satellite-based climatology of low-level continental clouds in southern West Africa during the summer monsoon season. *Journal of Geophysical Research: Atmospheres*, 120(3), pp. 1186-1201.